

# Non-simultaneity in two-photon coincidence spectroscopy

L. Horvath, B. C. Sanders and B. F. Wielinga

*Department of Physics, Macquarie University, Sydney, New South Wales 2109, Australia*  
(October 28, 2018)

Photon coincidence spectroscopy relies on detecting multiphoton emissions from the combined atom-cavity system in atomic beam cavity quantum electrodynamics experiments. These multiphoton emissions from the cavity are nearly simultaneous approximately on the cavity lifetime scale. We determine the optimal time for the detection window of photon pairs in two-photon coincidence spectroscopy. If the window time is too short, some photon pairs will not be detected; if the window time is too long, too many nearly coincident independent single photons will be falsely interpreted as being a photon pair.

42.50.Ct, 42.50.D

## I. INTRODUCTION

Cavity quantum electrodynamics (CQED) has continued to develop rapidly, driven both by recent experimental successes and by the promise of exciting new applications. Advances in atom cooling techniques, as well as development of high-Q optical cavities with large dipole coupling, have enabled testing of the strong-coupling regime of CQED [1]. Single-atom experiments are now feasible [2,3], and the possibility of trapping atoms in optical cavities is tantalisingly close [4]. Potential applications include quantum logic gates [5].

Applications of CQED rely critically on the quantum effects, namely the entanglement between the field degree of freedom and the internal electronic state of the atom [6,7]. This entanglement is not only challenging to achieve, it is also difficult to probe. In the optical regime of CQED, photon coincidence spectroscopy (PCS) has been proposed as a feasible and unambiguous method for detecting genuine quantum effects in CQED. This technique employs a multichromatic driving field acting on the combined atom-cavity system and detects multiphoton decays by detecting photon coincidences in the cavity output field [6,8,9].

A difficulty arises in determining whether emitted photons are coincident or not. Let us consider a single two-level atom (2LA) coupled to a single mode of an optical cavity, and  $\omega$  is the angular frequency of both the cavity mode and the 2LA. Multi-atom effects can be ignored provided that the atomic density is sufficiently small [10]. In the electric dipole and rotating-wave approximations, the Hamiltonian is

$$H(g) = \omega(\sigma_z + a^\dagger a) + ig(\mathbf{r})(a^\dagger \sigma_- - a \sigma_+) \quad (1.1)$$

with  $\mathbf{r}$  the position of the atom,  $g(\mathbf{r})$  the position-dependent dipole coupling strength,  $a$  and  $a^\dagger$  the annihilation and creation operators for photons in the cavity field,  $\sigma_+$ ,  $\sigma_-$ , and  $\sigma_z$  the 2LA raising, lowering and inversion operators, respectively, and  $\hbar = 1$ . The spectrum for this Hamiltonian is depicted in Fig. 1 and is the well-known Jaynes-Cummings spectrum, or ‘ladder’ [11]. The ‘dressed states’ of the combined atom-cavity system are designated by the lowest-energy state

$$|0\rangle \equiv |0\rangle_{\text{cav}} \otimes |\mathbf{g}\rangle_{\text{atom}}, \quad (1.2)$$

and, for  $n$  a positive integer,

$$|n\rangle_{\pm} \equiv \frac{i}{\sqrt{2}} (|n-1\rangle_{\text{cav}} \otimes |\mathbf{e}_{\text{atom}}\rangle \pm i|n\rangle_{\text{cav}} \otimes |\mathbf{g}_{\text{atom}}\rangle), \quad (1.3)$$

where  $|n\rangle$  is the Fock state of the cavity mode and  $|\mathbf{g}\rangle$  ( $|\mathbf{e}\rangle$ ) is the ground (excited) state of the 2LA.

Here we are concerned with two-photon coincidence spectroscopy (2PCS) which proceeds, first by driving the atomic beam with a bichromatic field which causes two-photon excitation to the second couplet of the JC ladder, followed by two-photon decay from the atom-cavity system. The objective is to count photon pairs emitted from the cavity as the frequencies of the driving field are varied. When the sum frequency is  $2\omega \pm \sqrt{2}g$ , we expect to see a resonantly enhanced two-photon count rate (2PCR). Of course,  $g$  is a random variable due to beam fluctuations, and this leads to inhomogeneous broadening. Despite these difficulties, 2PCS appears to be a feasible method for detecting the characteristic splitting in the JC model [6,8]. However, improvements in the procedure are important to ensure that the detection process is optimised.

In the following analysis we investigate the appropriate window time for counting photon pairs. Photon pairs are not emitted from the cavity simultaneously due to the randomness of photoemission from an optical cavity. The detection of a photon pair thus depends on identifying a window time  $\tau_w$  such that, for two photons detected with temporal separation  $t$  such that  $t < \tau_w$ , the two photons are deemed to be members of a pair, and, if  $t > \tau_w$ , are deemed to be independent single photons (not members of a pair). Here we determine the optimal window time  $\tau_{\text{opt}}$  which maximises the counting rate of genuine pairs relative to the rate of false pair counts.

## II. THE MASTER EQUATION

The Hamiltonian (1.1) for the combined atom-cavity system ignores the driving field emission of photons from the system. The Hamiltonian is useful in so far as it yields the spectrum for the combined atom-cavity system, but the full quantum master equation is necessary to calculate the quantities relevant to experiments, namely the two-photon count rate (2PCR). The experiment proceeds by measuring the 2PCR as a function of the bichromatic driving field's scanning field frequency.

Two-photon excitation is provided by driving the atom directly with a bichromatic field, characterised by the time-dependent variable

$$\mathcal{E}(t) = \mathcal{E}_1 e^{-i\omega_1 t} + \mathcal{E}_2 e^{-i\omega_2 t}. \quad (2.1)$$

The angular frequency  $\omega_1$  is fixed and resonantly excites the atom-cavity system from the ground state  $|0\rangle$  to the excited state  $|1\rangle_-$  for the subensemble  $g = g_f$ . That is, provided that

$$g_f = \omega - \omega_1, \quad (2.2)$$

the bichromatic driving field will resonantly excite the subensemble of atom-cavity systems for which  $g = g_f$ . Of course subensembles for which  $g \neq g_f$  can also be excited, but these excitations are non-resonant and hence less significant. The second frequency,  $\omega_2$ , is scanned over a particular frequency range. The purpose of the second component of the bichromatic field is to excite to one of the two states in the second couplet of the Jaynes-Cummings ladder, namely  $|2\rangle_{\pm}$ . Thus, the range of scanning frequencies for  $\omega_2$  must include the  $|1\rangle_- \longleftrightarrow |2\rangle_{\pm}$  transition frequencies,

$$\omega \pm (\sqrt{2} \mp 1)g, \quad (2.3)$$

respectively.

The amplitudes of the two chromatic components must be large enough to ensure sufficient occupation of the excited state but not large enough that significant Stark shifting or nonnegligible occupation of the higher-order states occurs. Enhanced rates of photon pair detection are then sought as the scanning frequency  $\omega_2$  is varied. The enhanced 2PCR occurs at the resonances shown in Fig. 1.

In addition to a driving term, loss terms must also be included. The Born-Markov approximation is applied to both radiation reservoirs: the reservoir for the field leaving the cavity and the reservoir for direct fluorescence of the 2LA from the sides of the cavity. The cavity damping rate is  $\kappa$ , and the emission rate into free space is  $\gamma$ , where  $\gamma$  is the inhibited spontaneous emission rate due to the restriction of modes by the cavity. The master equation [8] can be expressed as  $\dot{\rho} = \mathcal{L}\rho$  for  $\mathcal{L}$  the Liouvillean superoperator. More specifically the Liouvillean superoperator can be expressed as the sum of a time-independent Liouvillean operator, a time-dependent Liouvillean operator and a 'jump' term. By defining  $\delta = \omega_2 - \omega_1$ , in the rotating picture of  $\mathcal{E}_1$  the master equation is

$$\dot{\rho}(t; \delta, g) = [\mathcal{L}(g) + \mathcal{L}(t; \delta) + \mathcal{J}] \rho(t; \delta, g) \quad (2.4)$$

for

$$\begin{aligned} H_{\text{eff}}(g) = & (\omega - \omega_1) (\sigma_z + a^\dagger a) + ig(a^\dagger \sigma_- - a \sigma_+) \\ & + i\mathcal{E}_1 (\sigma_+ - \sigma_-) - i\kappa a^\dagger a - i(\gamma/2) \sigma_+ \sigma_- \end{aligned} \quad (2.5)$$

a non-Hermitian Hamiltonian, the first term is

$$\mathcal{L}(g)\rho = -i \left[ H_{\text{eff}}(g)\rho - \rho H_{\text{eff}}^\dagger(g) \right], \quad (2.6)$$

the time-dependent term is

$$\mathcal{L}(t; \delta)\rho = \mathcal{E}_2 [e^{-i\delta t}\sigma_+ - e^{i\delta t}\sigma_-, \rho], \quad (2.7)$$

and the jump term is

$$\mathcal{J}\rho = \gamma\sigma_-\rho\sigma_+ + 2\kappa a\rho a^\dagger. \quad (2.8)$$

The atom-field coupling strength  $g$  depends on the atomic position  $\mathbf{r}$ . Provided that the atoms move sufficiently slowly through the cavity [6,8], the atom can be treated as if it were at rest at some randomly located position  $\mathbf{r}$ . The interaction of the atom with the cavity is then described by the master equation in the asymptotic large time ( $t \rightarrow \infty$ ). As the position  $\mathbf{r}$  is a randomly varying quantity, the value of the coupling strength  $g$  itself is also random. Hence, a coupling strength distribution  $P(g)$  can be constructed [8]. The resultant density matrix is given by

$$\rho(t; \delta) = \int_{Fg_{\max}}^{g_{\max}} P(g)\rho(t; \delta, g)dg \quad (2.9)$$

where  $g_{\max}$  is the coupling strength at a cavity node and  $Fg_{\max}$  is the effective lower bound cut-off for the coupling ( $0 < F < 1$ ). The effect of averaging over  $P(g)$  is an inhomogeneous spectral broadening. This broadening is due to atomic position variability. In Fig. 2 two typical distributions  $P(g)$  are depicted, one for the case of a uniformly distributed atomic beam entering the cavity and the second for an atomic beam initially passing through a rectangular mask [8]. In both cases we assumed a single-mode cavity supporting a TEM<sub>00</sub> mode.

For a bichromatic driving field, the density matrix (2.9) does not settle to a steady state value. The time-dependence of the density matrix in the long-time limit can be treated by making a Bloch function expansion of the density matrix [8]. In the Bloch function expansion, the density matrix is written as the sum

$$\rho(t) = \sum_{N=0}^{\infty} \rho_N(t)e^{iN\delta t} \quad (2.10)$$

with  $\rho_N(t)$  time-dependent matrices. In the long-time limit,  $\dot{\rho}_N \approx 0$  and  $\rho_N$  can thus be regarded as time-independent. As the photocount integration time is expected to be long compared to the frequency  $\delta$ , it is reasonable to approximate  $\rho(t)$  by truncating the expansion (2.10).

### III. THE TWO-PHOTON COUNT RATE

The two-photon count rate (2PCR) can be obtained in more than one way. Ideally one would have a perfectly efficient photodetector which detects all photons leaving one side of the cavity. The photodetector would then provide a complete record of photon emissions from the cavity as a function of  $t$ . A perfect coincidence would then arise as two simultaneously detected photons at some time  $t$ . However, there are two problems. One problem is that there does not exist a perfectly efficient photodetector. Therefore, some pairs of photons are observed as single-photon emissions because one member of the pair escapes observation. In fact some pairs are missed altogether because both photons escape detection. The other problem concerns the detection of two simultaneously created photons. Although created simultaneously, the emission from the cavity is not simultaneous due to the randomness of the emission time which is characterised by the cavity lifetime  $1/\kappa$ .

A better and more accurate way to describe two-photon detections is to employ the 2PCR. To begin with, we consider two photons to be coincident provided that they arrive within a time interval  $\tau_w$ , the ‘window time’. The choice of window time is not obvious, and it is our aim here to determine what the window time should be. As the two simultaneous photons can be separated by a time of order  $\kappa^{-1}$ , as discussed above, the window time  $\tau_w$  might be expected to be on the order of  $\kappa^{-1}$ . However, our purpose here is to consider the choice of  $\tau_w$  in detail and to identify the optimal choice of window time  $\tau_w$  which will produce the best measure of the 2PCR.

The choice of optimal window time is further complicated by the method of detecting nearly simultaneous photons. In the ideal case discussed above of a perfect photodetector yielding a record of all photon emissions from the cavity, one can then define a two-photon event as taking place if a second photon arrives between times  $t_0$  and  $t_0 + \tau_w$ , *conditioned* on a photodetection at time  $t_0$ . We refer to this rate as the *conditional* 2PCR and define this rate to be

$$\begin{aligned} \Delta_{\text{con}}^{(2)}(\delta, g, \tau_w) \equiv & \lim_{t_0 \rightarrow \infty} \frac{1}{\tau_w} \int_{t_0}^{t_0 + \tau_w} dt \\ & \times \langle : \hat{n}(t_0)\hat{n}(t_0 + t) : \rangle (\delta, g). \end{aligned} \quad (3.1)$$

The number operator in eq (3.1) is defined as  $\hat{n}(t) \equiv \hat{a}^\dagger(t)\hat{a}(t)$ , and ‘:.’ refers to normal ordering. The averaging is performed for the density matrix of eq (2.4). The conditional 2PCR for a window time  $\tau_w = \kappa^{-1}$  was used in the quantum trajectory analysis of PCS in Ref. [6].

Another natural way to measure the 2PCR is by counting all photon pairs defined as being separated by an interval less than  $\tau_w$ . This 2PCR is referred to as the *unconditional* 2PCR and does not rely on starting the count for the second photon conditioned on detecting the first photon. The definition of the unconditional 2PCR is

$$\Delta_{\text{unc}}^{(2)}(\delta, g, \tau_w) = \lim_{t_0 \rightarrow \infty} \frac{2}{\tau_w^2} \int_{t_0}^{t_0 + \tau_w} dt' \int_{t_0}^{t'} dt \times \langle : \hat{n}(t) \hat{n}(t') : \rangle (\delta, g). \quad (3.2)$$

As shown in Appendix A, this expression can be simplified to read

$$\Delta_{\text{unc}}^{(2)}(\delta, g, \tau_w) = \frac{2}{\tau_w^2} \int_0^{\tau_w} du \int_0^u dw \times \langle : \hat{n}(0)\hat{n}(w) : \rangle (\delta, g). \quad (3.3)$$

We solve analytically for two extreme cases in Appendix A. The window time can be extremely long ( $\kappa\tau_w \gg 1$ ), yielding expression (A3), or extremely short ( $\kappa\tau_w \ll 1$ ), yielding expression (A4) for both conditional and unconditional 2PCR. The short window time ( $\tau_w \rightarrow 0$ ) was the basis of the analysis of 2PCS in Ref. [8]. In this treatment both the conditional and unconditional 2PCR at time  $t$  is approximated by  $\langle : \hat{n}^2(t) : \rangle$ . In the long-time limit the 2PCR is dominated by Poissonian statistics.

#### IV. THE OPTIMAL WINDOW TIME

The choice of optimal window time  $\tau_{\text{opt}}$  depends on the technique for observing two-photon coincidences, but another factor must also be considered. The purpose of 2PCS is to observe two-photon decay resonances from the combined atom-cavity system. As explained in Refs [6,8], there are three peaks in the 2PCR as a function of the scanning frequency  $\delta$ . These peaks are shown in Fig. 3 as a function of the normalised scanning field frequency

$$\tilde{\delta} = \frac{\omega_2 - \omega}{\omega - \omega_1}. \quad (4.1)$$

The choice of  $\tau_w$  will depend on which peak is being observed. However, the best peak for observing a two-photon decay resonance occurs for

$$\tilde{\delta} = 1 + \sqrt{2}. \quad (4.2)$$

This resonance corresponds to the transition  $|1\rangle_- \longleftrightarrow |2\rangle_+$ . This peak does not occur in a semiclassical description of intensity correlations in the cavity output field and therefore serves as a signature of a genuine quantum field effect in CQED. Moreover, this peak can be observed without the added complication of having to perform the experiment twice, once with a bichromatic field and once again with a monochromatic field, in order to perform the signal enhancement technique of background subtraction [6,8]. Finally detection of this peak is the most feasible of the three dominant peaks in the two-photon spectrum. Hence, we consider specifically  $\tau_w$  for this peak at  $\tilde{\delta}$  given by eq (4.2).

In Fig. 3 we observe that the 2PCR peak sits on a background 2PCR which is largely independent of  $\tilde{\delta}$  and occurs at  $\langle : \hat{n}^2 : \rangle \approx 2.1 \times 10^{-5}$ . Let us characterise the quality of this 2PCR peak by the ratio of the peak height to the height of the background 2PCR. We can understand this ratio in terms of signal to noise, where signal is the 2PCR from the sought-for two-photon decay events, and the background noise corresponds to two-photon decays arising from unwanted off-resonance two-quantum excitations and decay events. The peak-to-valley ratio (PVR) is determined by the height of the peak to the height of the background (or valley) 2PCR. The optimal window time  $\tau_w = \tau_{\text{opt}}$  is defined such that the PVR for this 2PCR is maximal. That is, either a larger or a smaller choice of the window time would reduce the value of the PVR making the peak more difficult to detect.

There are other concerns besides the PVR in choosing the window time. For example, choosing a much shorter window time could improve the PVR but also lengthen the run time of the experiment in order to accumulate enough signal. That is, the absolute height of the peak is also a matter of concern in determining the feasibility of the

experiment and is determined by the allowable timescale of the experiment. The minimum height would need to be on the order of  $T^{-1}$  for  $T$  the timescale of the data collection.

The PVR is obtained numerically. The matrix continued fraction method is used to solve the master equation to determine the peak height. The background, or valley, can be solved analytically though by treating the detuning of the scanning field as large. The details are provided in Appendix B.

The 2PCR for large  $\tilde{\delta}$  is given by expressions (B2) and (B5). The peak-to-valley ratio 2PCR is thus

$$\text{PVR}_\xi = \frac{\Delta_\xi^{(2)}(\tilde{\delta}, g, \tau_w)}{\left(\Delta_o^{(2)}\right)_\xi(g, \tau_w)} \quad (4.3)$$

where  $\xi \in \{\text{con}, \text{unc}\}$ . In Fig. 4 surface plots of the PVR *vs*  $g$  and  $\tau_w$  reveals that the PVR increases as  $g$  decreases. This is due to the background signal of two-photon coincidences for  $\tilde{\delta}$  large becoming negligible as shown in Fig. 3. Although the PVR improves as  $g$  decreases, the signal of two photon coincidences within the window time  $\tau_w$  decreases. This decrease is due to the fact that the resonant frequency for the transition  $|0\rangle \leftrightarrow |1\rangle_-$  is  $\omega - g$ , but we have constrained the pump field frequency by (2.2). Hence, as  $g$  decreases, the pump field drives the system more and more off resonance. The window time  $\tau_w$  for achieving the optimal PVR is an order of magnitude smaller than  $\kappa^{-1}$ . The optimal time  $\tau_{\text{opt}}$  exhibited in Fig. 5 is a function of coupling strength and in Fig. 6 is a function of  $\gamma/\kappa$  (averaged over  $P(g)$ ).

We are concerned specifically with the 2PCR and the PVR for the system with a coupling constant distribution based on the TEM<sub>00</sub> mode [6,8]. The coupling strength distribution is depicted in Fig. 2, and we treat the masked beam case which enhances the large-coupling effect.

In Fig. 7 we present the PVR for the density matrix  $\rho$  of expression (2.9), averaged over  $P(g)$ . There is a peak of the PVR for each  $g/\kappa$  given by  $\tau_w = \tau_{\text{opt}}$  (the optimal time window for observing the peak (4.2)). These values of  $\tau_{\text{opt}}$  are plotted in Fig. 5 for  $0 \leq g/\kappa \leq 10$  for a range of values of  $\gamma$ . Of particular interest here is the very weak dependence of  $\tau_{\text{opt}}$  on  $\gamma$  where  $\gamma$  is varied by a factor of 20. Moreover,  $\tau_{\text{opt}}$  is generally decreasing as  $g/\kappa$  increases.

## V. DISCUSSION

In Fig. 7 we observe a maximum of the PVR for each of the assumed  $P(g)$  in Fig. 2. This peak occurs at  $\kappa\tau_{\text{opt}} \approx 0.111$  for the conditional 2PCR and at  $\kappa\tau_{\text{opt}} \approx 0.135$  for the unconditional 2PCR. We can understand the location of these peaks by referring to Fig. 5.

In Fig. 5(a) the values of  $\kappa\tau_{\text{opt}}$  for the conditional 2PCR are predominantly between 0.11 and 0.16, but the value of  $\kappa\tau_{\text{opt}}$  in the vicinity of  $g/\kappa = 9$  is between 0.05 and 0.11. Due to the resonance condition (2.2) this region of the  $\kappa\tau_{\text{opt}}$  *vs*  $g/\kappa$  curve is more significant.

Hence, the dependence of  $\tau_{\text{opt}}$  on  $\gamma$  as depicted in Fig. 6 is dominated by the  $g/\kappa = 9$  region of Figs. 5. Similarly, we can estimate the precise value of  $\tau_{\text{opt}}$  for the unconditional 2PCR from the dashed line of Fig. 6 in the context of the values of  $\tau_{\text{opt}}$  in Fig. 5(b).

The linear dependence of  $\tau_{\text{opt}}$  on  $\gamma$ , as seen in Fig. 6 yields a correlation of 0.9983 for the conditional 2PCR, and a correlation of 0.9995 for the unconditional 2PCR. In the conditional case

$$\kappa\tau_{\text{opt}} \approx -(1.4 \times 10^{-3})\gamma/\kappa + 0.11 (\text{con}), \quad (5.1)$$

and in the unconditional case

$$\kappa\tau_{\text{opt}} \approx -(2.1 \times 10^{-3})\gamma/\kappa + 0.14 (\text{unc}). \quad (5.2)$$

The low values of the slopes are indicative of the weak dependence on  $\gamma$ . Formulae (5.1) and (5.2) can be used to fine-tune the choice of optimal window time, and the linear relationship simplifies the task of interpolating to obtain  $\tau_{\text{opt}}$ .

## VI. CONCLUSIONS

We have determined expressions for the optimal window time  $\tau_{\text{opt}}$  for both conditional and unconditional 2PCR. These expression provide an optimal PVR for the 2PCR peak at  $\tilde{\delta} = 1 + \sqrt{2}$  corresponding to the  $|1\rangle_- \rightarrow |2\rangle_+$  transition. Although we have determined  $\tau_{\text{opt}}$  for certain parameters and for the coupling-strength distribution  $P(g)$

(solid line of Fig. 2), the algorithm presented here is sufficiently general to allow calculation of  $\tau_{\text{opt}}$  for other parameters and other coupling-strength distributions. In general  $\tau_{\text{opt}}$  is smaller than  $\kappa^{-1}$  by an order of magnitude for both the conditional and unconditional 2PCR. There is some dependence on  $\gamma$ , but this dependence is weak and is close to linear in the cases studied here.

Analyses of optimal window times are aided by studies of  $\tau_{\text{opt}}$  for particular values of  $g$ , that is, for the coupling-strength distribution  $P(g)$  corresponding to  $\delta(g - g_0)$  for some  $g_0$ . These calculations provide good estimates of the optimal window time for general  $P(g)$ . A longer window time may be desirable, however, if the timescale for collecting enough data is not experimentally feasible. A compromise between the two objectives of optimising the PVR and of accumulating sufficient data to produce a large peak height may be necessary.

An important technique discussed in Refs. [6,8] was background subtraction. The principle behind this method is to remove the unwanted two-photon off-resonance excitation to the second couplet. Background subtraction is particularly important to improve the PVR for 2PCR peaks. However, we choose to study detection of the most promising peak experimentally (4.2). In our simulations we determine the PVR for this peak both by performing background subtraction and without background subtraction, and we obtain plots in agreement with Figs. 4 and 7. These results confirm the assertion in Ref. [8] that “the resonance frequency lies outside the inhomogeneous line and the resonance should be resolved even in the presence of the two-photon background”. Hence, background subtraction is not necessary to obtain optimal window times for resolving the peak (4.2).

### ACKNOWLEDGEMENTS

Dr S. M. Tan has provided Matlab<sup>TM</sup> programs to us which was used initially to double check our simulations of the monochromatically driven Jaynes-Cummings system. We have benefited from valuable discussions with H. J. Carmichael, J. D. Cresser, Z. Ficek, K.-P. Marzlin, and S. M. Tan. This research has been supported by Australian Research Council Large and Small Grants and a Macquarie University Research Grant.

## APPENDIX: A: THE CONDITIONAL AND UNCONDITIONAL TWO-PHOTON COUNT RATE (2PCR)

In the long-time limit, the conditional two-photon count rate (2PCR) is given by

$$\Delta_{\text{con}}^{(2)}(\delta, g, \tau_w) = \frac{1}{\tau_w} \int_0^{\tau_w} dt \langle : \hat{n}(0)\hat{n}(t) : \rangle (\delta, g). \quad (\text{A1})$$

If the time window  $\tau_w$  is large, compared to  $\kappa^{-1}$  (the cavity lifetime), the two photons are highly decorrelated, and we can approximate

$$\langle : \hat{n}(0)\hat{n}(t) : \rangle (\delta, g) \longrightarrow \langle \hat{n}(0) \rangle^2 (\delta, g). \quad (\text{A2})$$

Thus,

$$\Delta_{\text{con}}^{(2)}(\delta, g, \tau_w) \longrightarrow \langle \hat{n}(0) \rangle^2 (\delta, g). \quad (\text{A3})$$

This count rate reflects the Poissonian nature of the count statistics for long window times. On the other hand, for  $\kappa\tau_w \ll 1$ , the correlation between photon pairs cannot be neglected. Hence, the count rate reduces to

$$\Delta_{\text{con}}^{(2)}(\delta, g, \tau_w) \longrightarrow \langle : \hat{n}^2(0) : \rangle (\delta, g) \quad (\text{A4})$$

which is the approximation employed in Ref [8].

Similarly, in the long-time limit, the unconditional 2PCR is

$$\Delta_{\text{unc}}^{(2)}(\delta, g, \tau_w) = \frac{2}{\tau_w^2} \int_0^{\tau_w} dt' \int_0^{t'} dt \langle : \hat{n}(t)\hat{n}(t') : \rangle (\delta, g). \quad (\text{A5})$$

This expression can be simplified as we show below. First we make the substitution  $u_{\pm} = (t' \pm t)/\sqrt{2}$ . We also introduce the notation  $d^2u = du_- du_+$  and let  $\nu$  be the union of the two regions  $\{0 < u_- < \tau_w/\sqrt{2}, 0 < u_+ < u_-\}$  and  $\{\tau_w/\sqrt{2} < u_- < \sqrt{2}\tau_w, 0 < u_+ < \sqrt{2}\tau_w - u_-\}$

This substitution transforms the above double integral into the sum of two double integrals:

$$\begin{aligned} \Delta_{\text{unc}}^{(2)}(\delta, g, \tau_w) &= \frac{2}{\tau_w^2} \int \int_{\nu} \left\langle : \hat{n} \left( \frac{u_+ - u_-}{\sqrt{2}} \right) \hat{n} \left( \frac{u_+ + u_-}{\sqrt{2}} \right) : \right\rangle (\delta, g) \\ &= \frac{2}{\tau_w^2} \int \int_{\nu} \left\langle : \hat{n}(0)\hat{n}(\sqrt{2}u_+) : \right\rangle (\delta, g). \end{aligned} \quad (\text{A6})$$

The advantage of this expression is that the two-time photon number correlation depends on only one term in the double integral instead of both terms in the double integral.

Greater simplification is possible and desirable for studying the short and long window time  $\tau_w$ . Substituting  $u_{\pm} = w_{\pm}/\sqrt{2}$  transforms eq (A6) to

$$\begin{aligned} \Delta_{\text{unc}}^{(2)}(\delta, g, \tau_w) &= \frac{1}{\tau_w^2} \left[ \int_0^{\tau_w} dw_- \int_0^{w_-} dw_+ \right. \\ &\quad \left. + \int_{\tau_w}^{2\tau_w} dw_- \int_0^{2\tau_w - w_-} dw_+ \right] \\ &\quad \langle : \hat{n}(0)\hat{n}(w_+) : \rangle (\delta, g) \end{aligned} \quad (\text{A7})$$

which reduces to

$$\begin{aligned} \Delta_{\text{unc}}^{(2)}(\delta, g, \tau_w) &= \frac{2}{\tau_w^2} \int_0^{\tau_w} du \int_0^u dw \\ &\quad \times \langle : \hat{n}(0)\hat{n}(w) : \rangle (\delta, g). \end{aligned} \quad (\text{A8})$$

For large ( $\tau_w \gg \kappa^{-1}$ ) and small ( $\tau_w \ll \kappa^{-1}$ ) window times  $\Delta_{\text{unc}}^{(2)}$  reduces identically to  $\Delta_{\text{con}}^{(2)}$  as shown in equations (A3) and (A4).

## APPENDIX: B: BACKGROUND OF CONDITIONAL AND UNCONDITIONAL 2PCR

For the scanning field far off resonance ( $\delta$  large), the time-dependent component of the Liouvillean (2.7) can be ignored. In the interaction picture, the master equation can be written as  $\dot{\rho} = \mathcal{L}\rho$  with  $\mathcal{L}$  time-independent. If  $\rho$  is expressed as a vector, then  $\mathcal{L}$  can be expressed as a complex matrix with  $\{-\lambda_n | n \in \mathcal{Z}_{N^2}\}$  the set of eigenvalues for  $N$  the number of levels in the Jaynes-Cummings ladder retained after truncation. The density matrix can be approximated by the sum

$$\rho(t) = \sum_{n=1}^{N^2} \rho_n e^{-\lambda_n(t-t_0)} \quad (\text{B1})$$

for  $\{\rho_n\}$  a set of time-independent  $N \times N$  matrices. Thus, the conditional 2PCR (3.1) can be written as

$$\begin{aligned} \left(\Delta_o^{(2)}\right)_{\text{con}}(g, \tau_w) &= c_0(g) + \frac{1}{\tau_w} \int_0^{\tau_w} dt \\ &\times \sum_{n=1}^{N^2} c_n(g) \exp[-\lambda_n(g)t] \\ &= c_0(g) + \sum_{n=1}^{N^2} \frac{c_n(g)}{\mu_n(g)} \left\{1 - e^{-\mu_n(g)}\right\}. \end{aligned} \quad (\text{B2})$$

with  $N^2$  scalar constants  $\{c_n(g)\}$  and  $N^2$  constants  $\{\mu_n(g)\}$  where

$$\mu_n(g) = \lambda_n(g)\tau_w \neq 0, \quad \text{Re}\{\lambda_n(g)\} \geq 0 \quad (\text{B3})$$

as well. In the long window time limit, we equate

$$c_0(g) = \lim_{\tau_w \rightarrow \infty} \left(\Delta_o^{(2)}\right)_{\text{con}}(g, \tau_w). \quad (\text{B4})$$

Expansion (B2) provides a useful method for calculating  $\left(\Delta_o^{(2)}\right)_{\text{con}}(g, \tau_w)$ . The function  $\left(\Delta_o^{(2)}\right)_{\text{con}}(g, \tau_w)$  is monotonically increasing because  $\partial \left(\Delta_o^{(2)}\right)_{\text{con}}(g, \tau_w) / \partial \tau_w > 0$  if  $\tau_w \rightarrow \infty$ . Thus,  $\partial \left(\Delta_o^{(2)}\right)_{\text{con}}(g, \tau_w) / \partial \tau_w \rightarrow 0$  as the function approaches the limit given by (B4).

In the same way, the unconditional 2PCR can be obtained:

$$\begin{aligned} \left(\Delta_o^{(2)}\right)_{\text{unc}}(g, \tau_w) &= c_0(g) + \frac{2}{\tau_w^2} \int_0^{\tau_w} du \int_0^u dw \\ &\times \sum_{n=1}^{N^2} c_n(g) \exp[-\lambda_n(g)w] = c_0(g) \\ &+ 2 \sum_{n=1}^{N^2} \frac{c_n(g)}{\mu_n(g)} \left\{ \frac{e^{-\mu_n(g)} - 1}{\mu_n(g)} + 1 \right\}. \end{aligned} \quad (\text{B5})$$

Thus, as in (B4), the long time limit reduces (B5) to  $c_0(g)$ .

- [1] R. J. Thompson, Q. A. Turchette, O. Carnal and H. J. Kimble, Phys. Rev. A, **57**, 3084 (1998).
- [2] C. J. Hood, M. S. Chapman, T. W. Lynn and H. J. Kimble, Phys. Rev. Lett. **80**, 4157 (1998).
- [3] H. Mabuchi, J. Ye and H. J. Kimble, J. Appl. Phys. B unpublished (1998).
- [4] A. S. Parkins and H. J. Kimble unpublished.



- [5] Q. A. Turchette, C. J. Hood, W. Lange, H. Mabuchi and H. J. Kimble, Phys. Rev. Lett. **75**, 4710 (1995).
- [6] H. J. Carmichael, P. Kochan, and B. C. Sanders, Phys. Rev. Lett. **77**, 631 (1996).
- [7] M. Brune, F. Schmidt-Kaler, A. Maali, J. Dreyer, E. Hagley, J. M. Raimond, and S. Haroche, Phys. Rev. Lett. **76**, 1800 (1996).
- [8] B. C. Sanders, H. J. Carmichael, B. F. Wielinga, Phys. Rev. A **55**, 1358 (1997).
- [9] L. Horvath, B. C. Sanders and B. F. Wielinga, J. Opt. B: Quant. and Semiclassical Opt. (accepted).
- [10] H. J. Carmichael and B. C. Sanders, Phys. Rev. A, (accepted).
- [11] E. T. Jaynes and F. W. Cummings, Proc. IEEE **51**, 89 (1963).

FIG. 1. Selection of two subpopulations of the inhomogeneously broadened Jaynes-Cummings (JC) system via distinct absorption paths. The ground state energy and the inhomogeneously broadened energy bands associated with the first, second and third coupler of the JC spectrum are shown.

FIG. 2. The scaled coupling strength distributions  $\kappa P(g)$  as a function of  $g/\kappa$  for single atoms passing through an optical cavity supporting a single TEM<sub>00</sub> mode. The solid curve corresponds to a typical distribution for a rectangular mask filtering the atomic beam. The dashed line corresponds to the absence of a mask.

FIG. 3. Spectrum of the simultaneous 2PCR (averaged over the coupling strength distribution  $P(g)$  shown with the solid line in Fig. 2) as a function of the normalised driving field frequency  $\tilde{\delta}$ .

FIG. 4. The peak-to-valley ratio of the (a) conditional ( $\text{PVR}_{\text{con}}$ ) and (b) unconditional ( $\text{PVR}_{\text{unc}}$ ) 2PCR over the scaled coupling strength  $g/\kappa$  and the scaled window time  $\kappa\tau_w$  for the scaled loss rate  $\gamma/\kappa = 2$ .

FIG. 5. The scaled optimal window time  $\kappa\tau_{\text{opt}}$  vs the scaled coupling strength  $g/\kappa$  for  $\diamond \gamma/\kappa = 0.2$ ,  $+ \gamma/\kappa = 2$ ,  $\square \gamma/\kappa = 5$ ,  $\times \gamma/\kappa = 7$  and  $\triangle \gamma/\kappa = 10$  for (a) the conditional and (b) the unconditional 2PCR.

FIG. 6. The scaled optimal window time  $\kappa\tau_{\text{opt}}$  vs the scaled loss rate  $\gamma/\kappa$  for the masked atomic beam. The symbol  $+$  corresponds to the conditional  $\tau_{\text{opt}}$  and  $\diamond$  to the unconditional  $\tau_{\text{opt}}$ . Linear regression methods yield the two lines. For the conditional case, the slope is  $-1.4 \times 10^{-3}$ , the intercept is 0.11, and the correlation coefficient is  $r = -0.9983$ . For the unconditional case, the slope is  $-2.1 \times 10^{-3}$ , the intercept is 0.14, and the correlation coefficient is  $r = -0.9995$ .

FIG. 7. The peak-to-valley ratio (PVR) of the conditional (solid line) and unconditional (dashed line) 2PCR (for the masked atomic beam) vs the scaled window time  $\kappa\tau_w$  for the scaled loss rate  $\gamma/\kappa = 2$ .

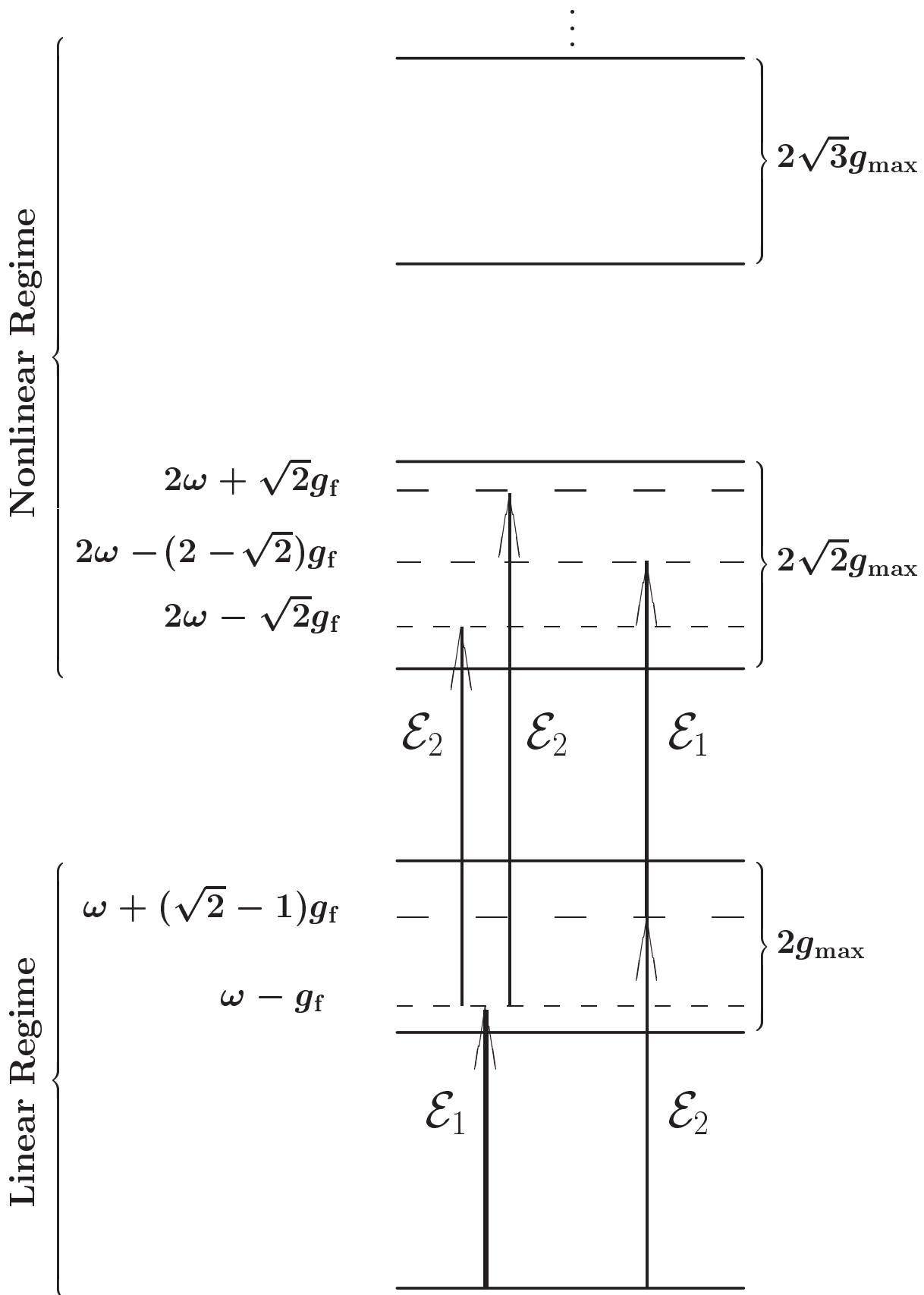


Fig. 1  
 Horvath et al.  
 Euro. Phys. J. D

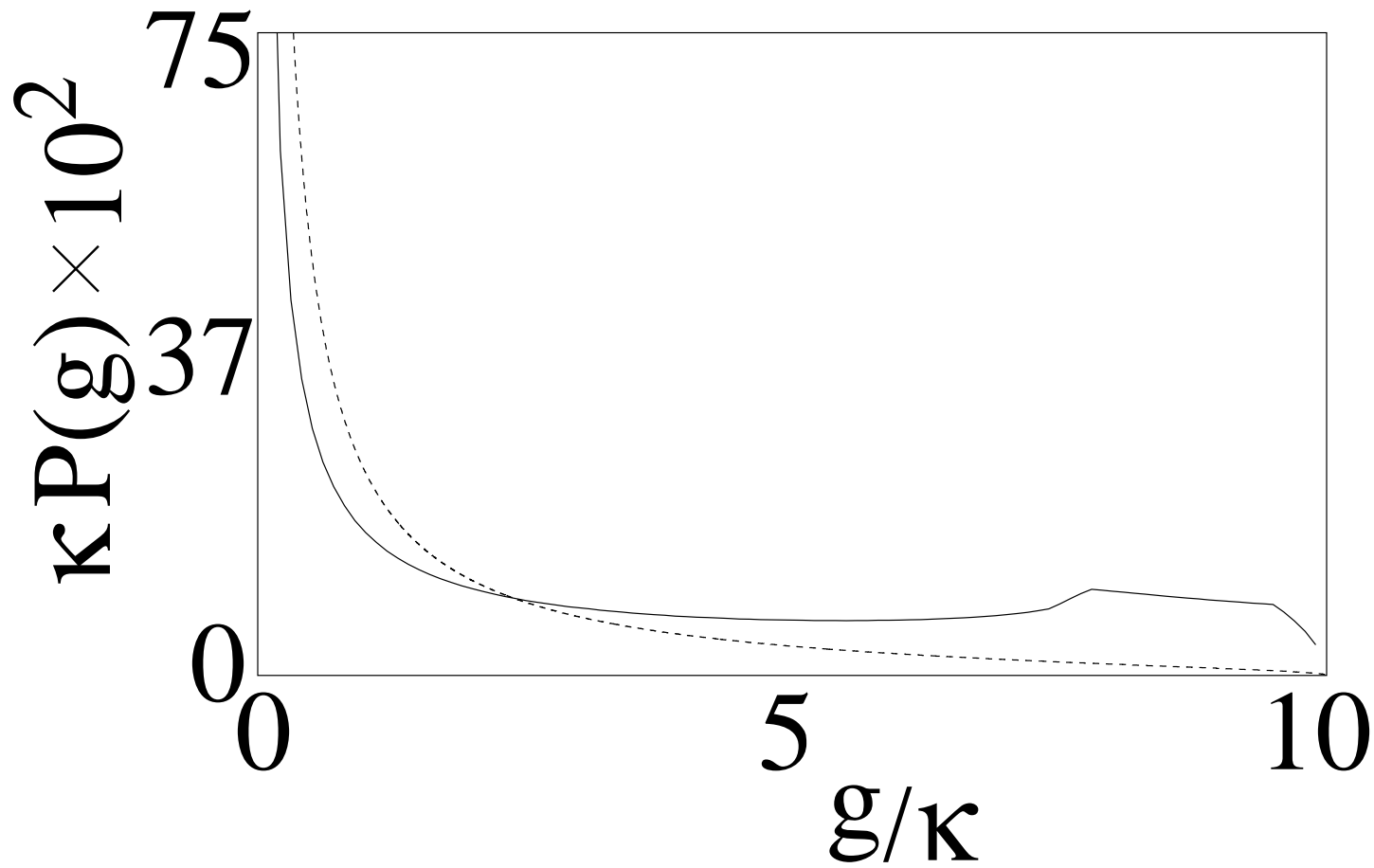


Fig. 2  
Horvath et al.  
Euro. Phys. J. D

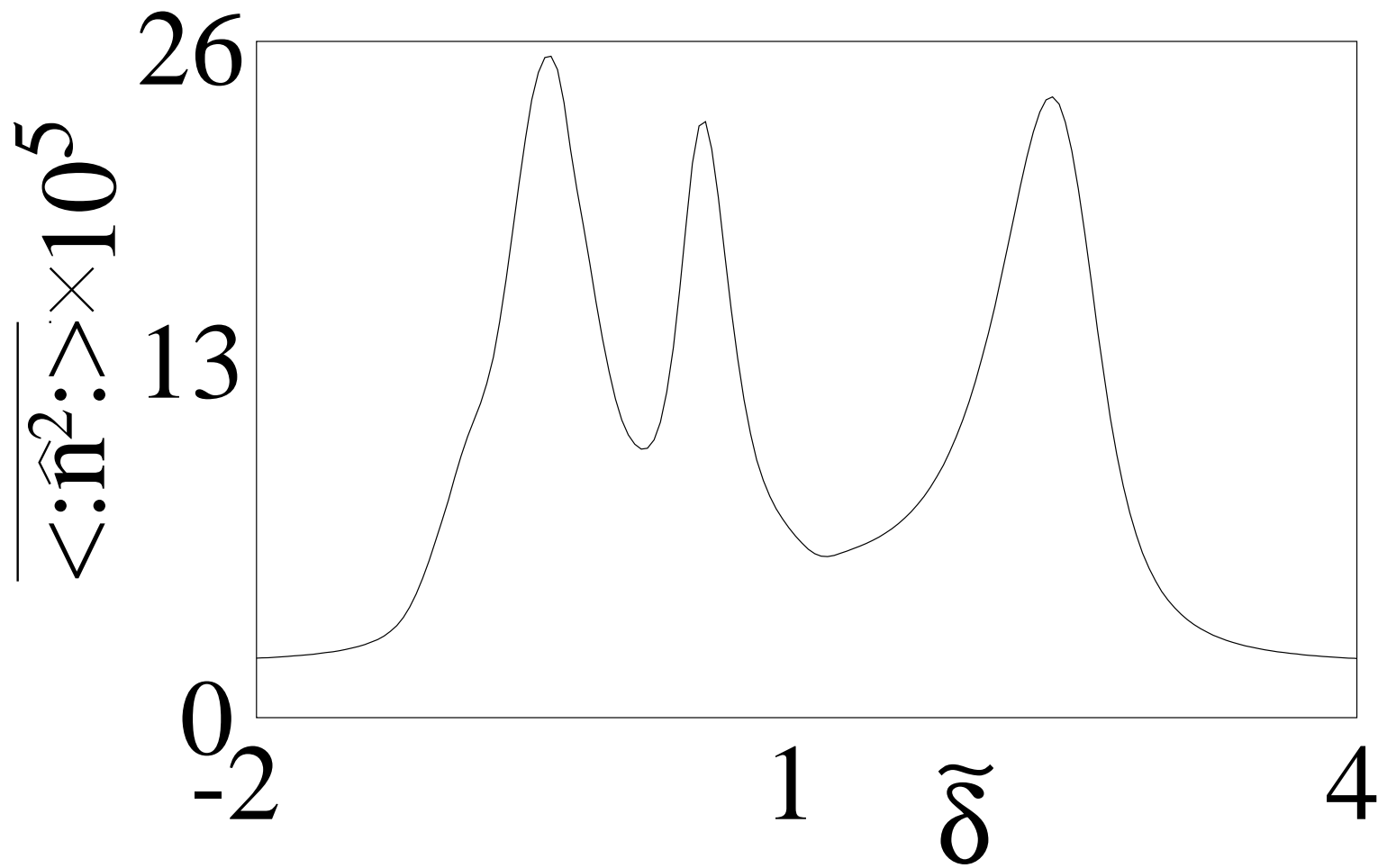
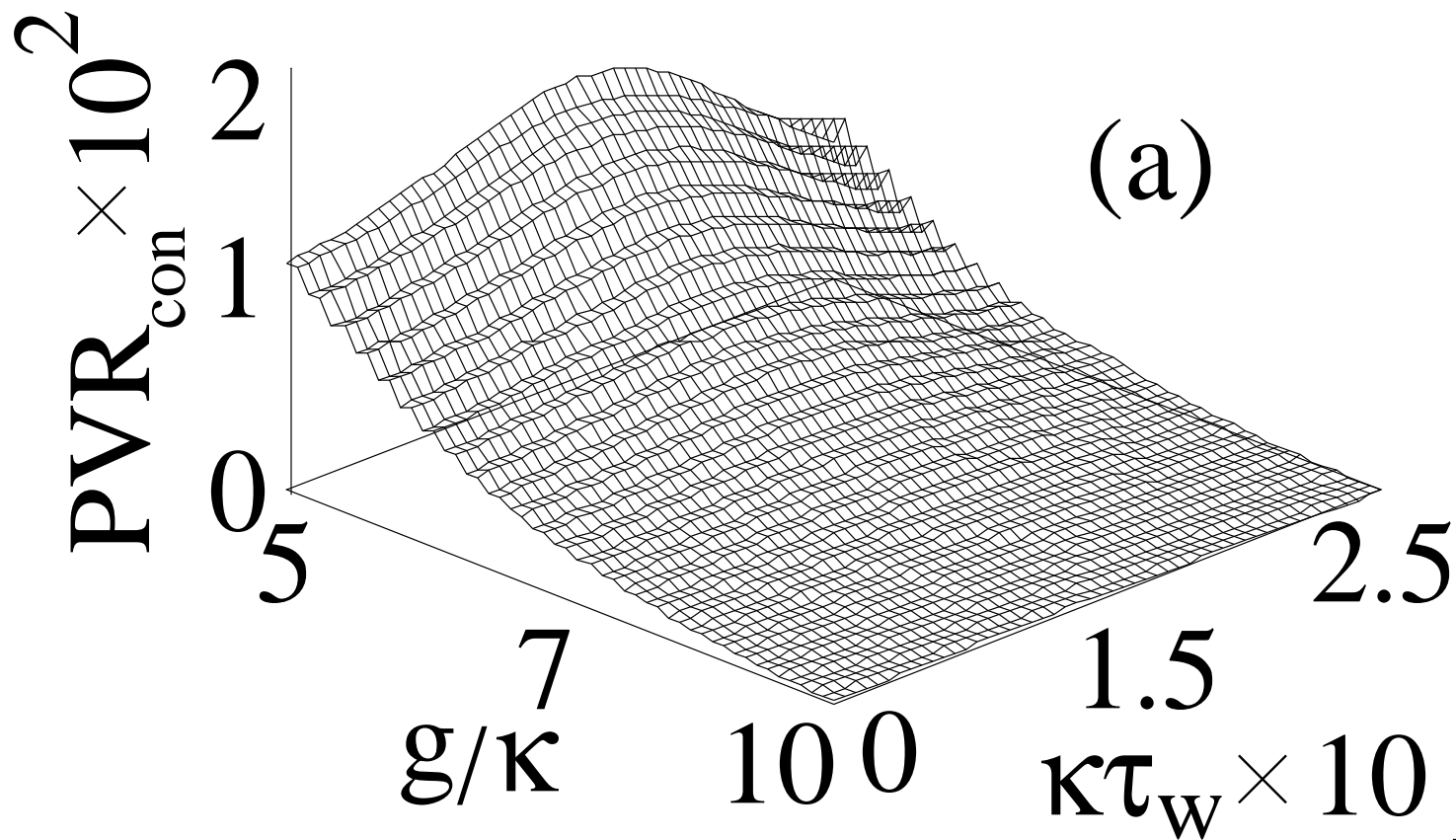


Fig. 3  
Horvath et al.  
Euro. Phys. J. D



(a)

Fig. 4(a)  
Horvath et al.  
Euro. Phys. J. D

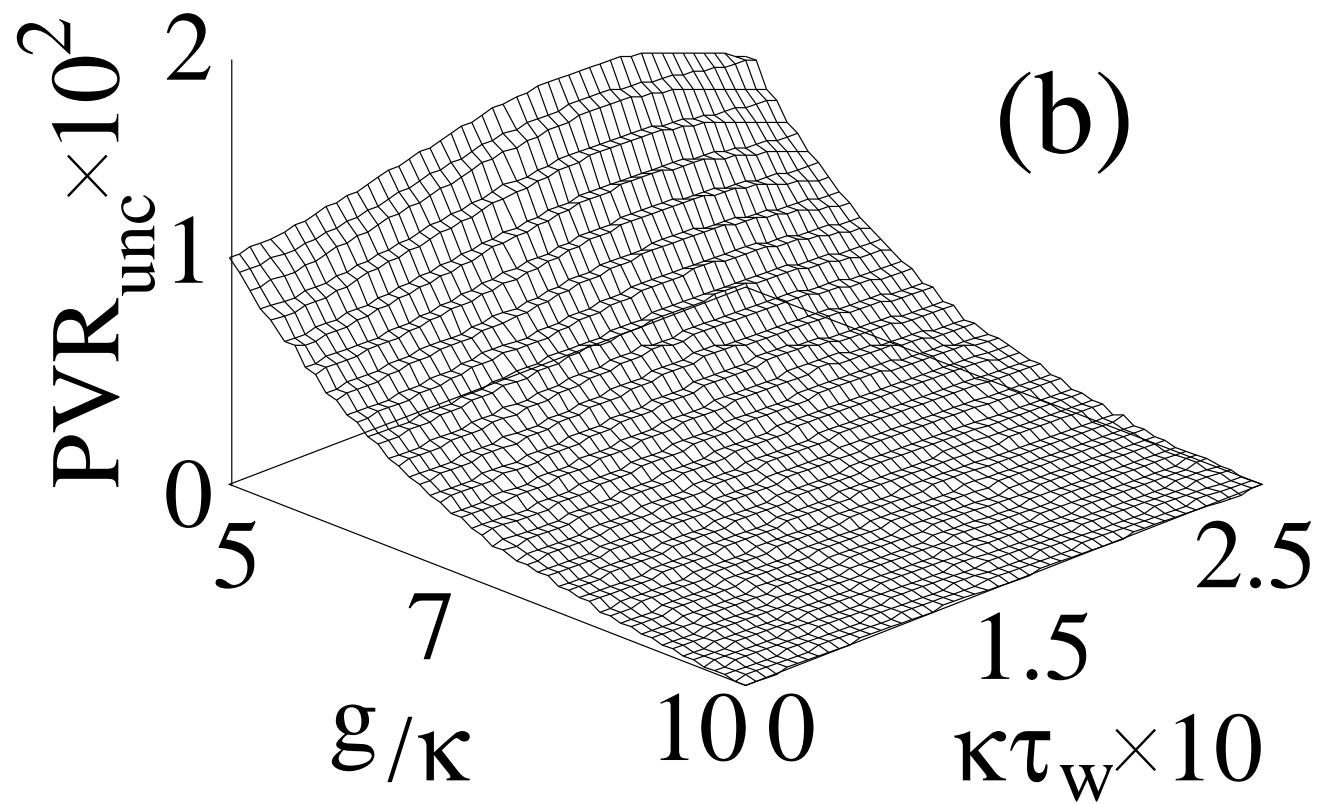


Fig. 4(b)  
Horvath et al.  
Euro. Phys. J. D

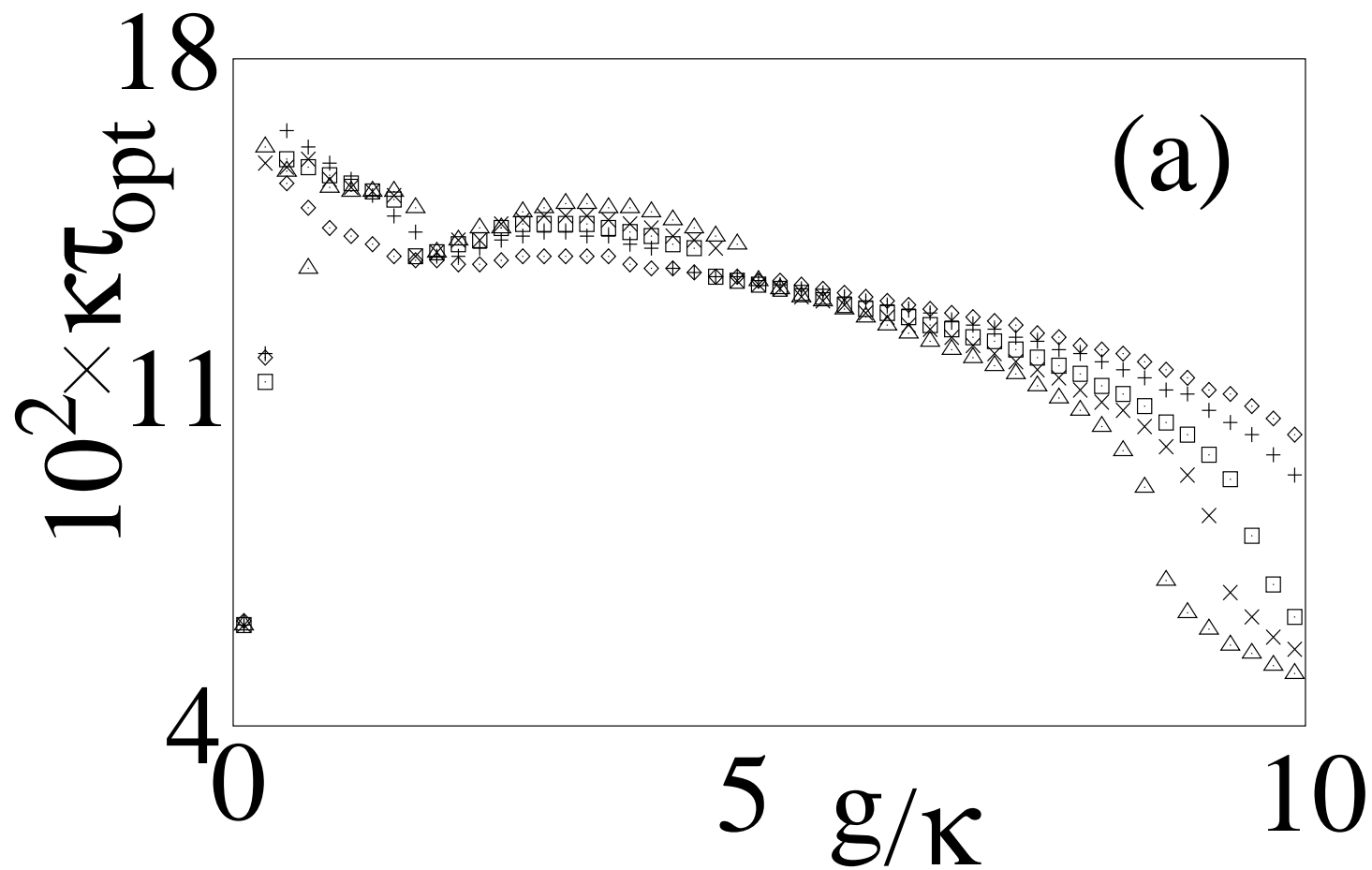


Fig. 5(a)  
Horvath et al.  
Euro. Phys. J. D



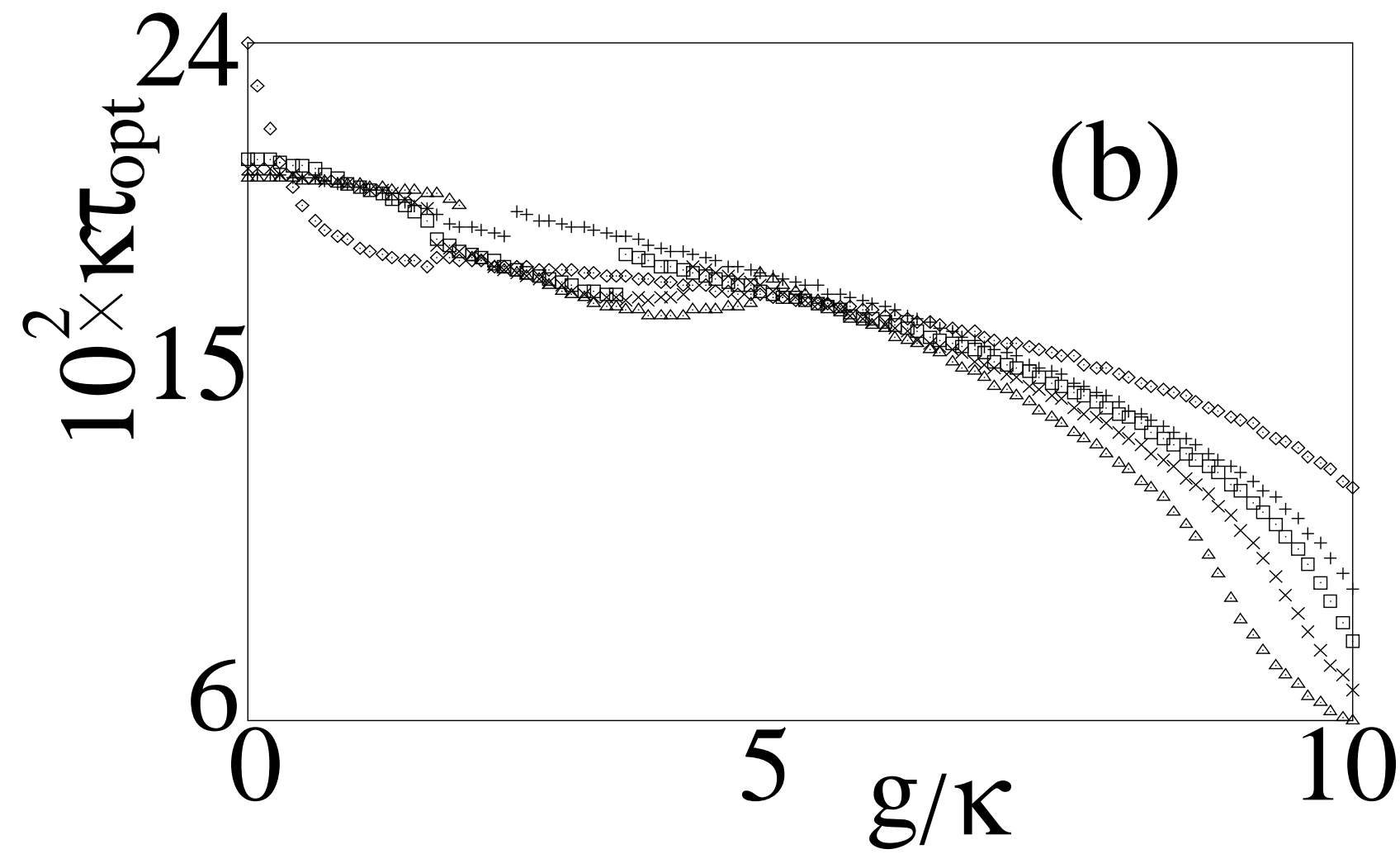


Fig. 5(b)  
Horvath et al.  
Euro. Phys. J. D

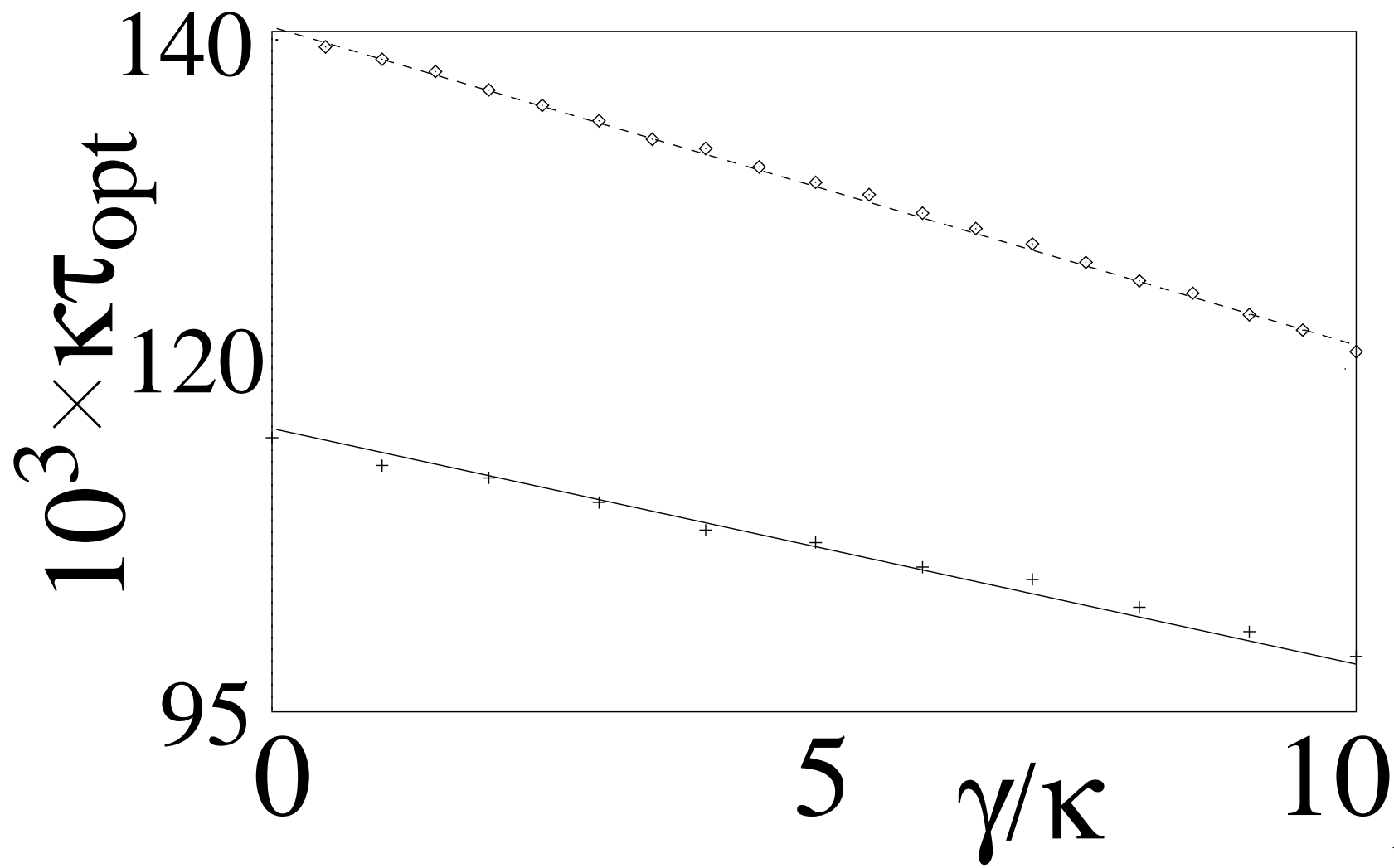


Fig. 6  
Horvath et al.  
Euro. Phys. J. D

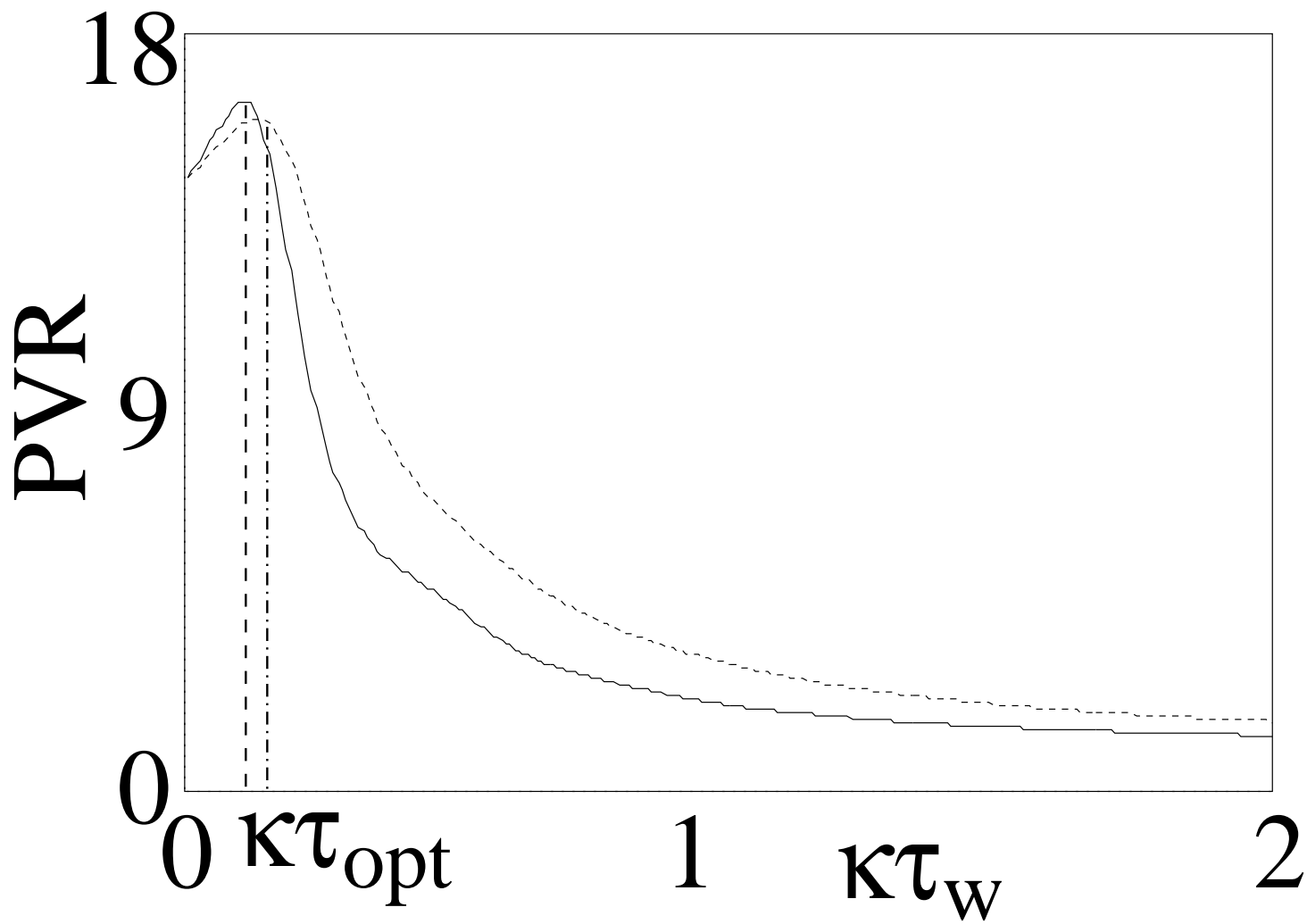


Fig. 7  
Horvath et al.  
Euro. Phys. J. D